Acta Oceanol. Sin., 2024, Vol. 43, No. 6, P. 15–31
https://doi.org/10.1007/s13131-023-2283-6
http://www.aosocean.com
E-mail: ocean2@hyxb.org.cn

The impact of typhoons on the biogeochemistry of dissolved organic matter in eutrophic bays in northwestern South China Sea

Xuan Lu[1, 2], Qibin Lao[1], Fajin Chen[1, 3, 4]*, Guangzhe Jin[1, 3, 4], Chunqing Chen[1], Qingmei Zhu[1, 3, 4]

[1] College of Ocean and Meteorology, Guangdong Ocean University, Zhanjiang 524088, China

[2] Polar and Marine Research Institute, College of Harbor and Coastal Engineering, Jimei University, Xiamen 361021, China

[3] Key Laboratory for Coastal Ocean Variation and Disaster Prediction, Guangdong Ocean University, Zhanjiang 524088, China

[4] Key Laboratory of Climate, Resources and Environment in Continental Shelf Sea and Deep Sea, Department of Education of Guangdong Province, Guangdong Ocean University, Zhanjiang 524088, China

Received 30 August 2023; accepted 7 December 2023

Abstract

Highly productive estuaries facilitate intense decomposition of dissolved organic matter (DOM) as a carbon source. However, the specific impacts of typhoons on DOM decomposition in eutrophic bays remain unclear. To address this issue, we investigated the spectral characteristics of DOM before and after Typhoon Ewiniar in Zhanjiang Bay, a eutrophic semi-enclosed bay in the northwestern South China Sea. The results revealed that intense microbial decomposition of DOM occurred during the pre-typhoon period because high nutrient inputs facilitated the mobilization of DOM in the bay. However, the intrusion of external seawater induced by the typhoon diluted the nutrient levels in Zhanjiang Bay, reducing the impact of microbial decomposition on DOM during the post-typhoon period. Nevertheless, the net addition of DOM occurred in Zhanjiang Bay during the post-typhoon period, possibly because of the decomposition of particulate organic matter (POM) and desorption of particulate matter. In addition, an increase in apparent oxygen utilization, a decrease in DO saturation and the reduced level of Chl *a* indicated that organic matter (OM) decomposition was enhanced and OM decomposition shifted to POM decomposition in Zhanjiang Bay after the typhoon. Overall, our study highlighted the shift in the intense OM decomposition from DOM to POM decomposition before and after typhoons in eutrophic bays, providing new insights into the response of typhoons to biogeochemistry.

Key words: dissolved organic matter, optical analyses, decomposition, typhoon, northwestern South China Sea

Citation: Lu Xuan, Lao Qibin, Chen Fajin, Jin Guangzhe, Chen Chunqing, Zhu Qingmei. 2024. The impact of typhoons on the biogeochemistry of dissolved organic matter in eutrophic bays in northwestern South China Sea. Acta Oceanologica Sinica, 43(6): 15–31, doi: 10.1007/s13131-023-2283-6

1 Introduction

Typhoons are extreme weathers that can alter physical processes and impact carbon and nitrogen cycles in the ocean (Lin et al., 2003; Li et al., 2022a; Lu et al., 2022a; Lao et al., 2023c, 2023b). Previous studies have demonstrated that nutrient inputs after a typhoon can trigger phytoplankton blooms, which enhance biological carbon sequestration in the ocean (as a carbon sink) (Lin et al., 2003; Lin, 2012; Li et al., 2022a). In contrast, our recent studies have revealed that the decomposition (as a carbon source) of organic matter (OM) is the dominant process, regardless of whether phytoplankton blooms occur after typhoons, due to the strong stirring effect of typhoons on the ocean (Chen et al., 2023; Zhou et al., 2021; Lu et al., 2022a; Lao et al., 2023a). Therefore, understanding the production and decomposition processes of nearshore OM induced by typhoons is essential for understanding both regional and global carbon cycle dynamics (Sobel et al., 2016; Balaguru et al., 2016; Wang et al., 2022).

Dissolved organic matter (DOM) contributes ~90% of the organic carbon in the global ocean, compared to particulate organic carbon (POC, only ~10%) (Chen et al., 2004; Jiao et al., 2010, 2011; Danhiez et al., 2017; Xiao et al., 2023). Microbially mediated refractory DOC (RDOC) has been stored in oceans for thousands of years and plays a crucial role in global carbon storage (Jiao et al., 2010, 2011; Wang et al., 2021a, 2021b; Qu et al., 2022). DOM levels can be influenced by both production and decomposition processes, with local productivity playing a role in production and heterotrophic microorganisms influencing decomposition (Jiao et al., 2010, 2011; Zhang et al., 2017). In general, high productivity results in high DOM levels in nearshore waters (Asmala et al., 2018; Zhao et al., 2021; He et al., 2023). In contrast, eutrophication in nearshore waters reduces the C/N and C/P ratios owing to the inputs of nitrogen (N) and phosphorus (P), thereby enhancing the bioactivity of DOC, which can be rapidly utilized by microorganisms, leading to rapid decomposition (Zweifel et al., 1993; Yuan et al., 2010; Jiao et al., 2011, 2018). However, changes in water mass mixing can alter the nutrient

Foundation item: The National Natural Science Foundation of China under contract Nos 42276047, 92158201 and U1901213; the Entrepreneurship Project of Shantou under contract No. 2021112176541391; and the Scientific Research Start-Up Foundation of Shantou University under contract No. NTF20006.

*Corresponding author, E-mail: fjchen@gdou.edu.cn

distribution (Lao et al., 2022a, 2023b), especially under the strong external forces of typhoons (Lao et al., 2023c). For example, seawater intrusion can dilute nutrients in coastal bays (Lao et al., 2022b), which may decrease DOM bioactivity (Jiao et al., 2011, 2018). Therefore, when assessing the contribution of DOC to marine carbon storage, it is crucial to consider its decomposition, which leads to carbon release (Jiao et al., 2010, 2011; Qu et al., 2022; He et al., 2022).

The cycling of DOM in estuaries and bays is inherently complex (Li et al., 2022b; He et al., 2022; Liu et al., 2020; Gao et al., 2019), involving diverse origins, such as offshore transport, *in situ* biotic production, and inputs from major land-based origins (He et al., 2010, 2022; Guo et al., 2014; Asmala et al., 2018). In addition, DOM in estuaries and bays is highly vulnerable to human activities (Zhao et al., 2021; Li et al., 2021; Lu et al., 2022b; He et al., 2022). Dynamic physical processes such as typhoons can significantly complicate the carbon cycling of DOM in nearshore waters (Hoge and Lyon, 2002; Conmy et al., 2009; Letourneau and Medeiros, 2019). However, the specific mechanisms by which DOM decomposition is affected by typhoons in eutrophic bays remain unclear.

Spectroscopic techniques are essential for investigating the origins and transformation processes of marine DOM (Loginova et al., 2016; Qu et al., 2020; Wang et al., 2017, 2021b). In recent years, spectroscopic techniques have been widely employed in estuaries and bays (Liu et al., 2020; Zhao et al., 2021; He et al., 2022; Lu et al., 2023). Parameters a_{254} and a_{325} are typically used to quantify the levels of chromophoric DOM (CDOM) within DOM (Wang et al., 2017, 2021b; Lu et al., 2023). Additionally, the molecular size of DOM can be characterized by spectral slopes such as $S_{275-295}$ (Helms et al., 2008; Guo et al., 2014). The intensity of the fluorescent component is described as fluorescent DOM (FDOM) (Guo et al., 2014; Wang et al., 2022). Indices such as the humic index (HIX), biotic index (BIX), and fluorescence index (FI) can be employed to assess DOM quality (Wang et al., 2017, 2021b; Lu et al., 2022b). More importantly, spectroscopic techniques provide an effective means for studying the decomposition process of DOM because humus-like FODM generally correlate with apparent oxygen utilization (AOU) in water columns, indicating an association between OM decomposition and oxygen consumption (Wang et al., 2021a; Qu et al., 2022; He et al., 2022; Xiao et al., 2023). Therefore, spectroscopic techniques can be effectively used to investigate the processes related to both the production and decomposition of DOM after typhoons.

The northwestern South China Sea (SCS) is frequently affected by typhoons (Wu et al., 2005; Zhou et al., 2021; Lu et al., 2022a), with approximately ten typhoons annually impacting this region (Chen et al., 2021). Therefore, it is an ideal area for studying the response of dynamic DOM processes to typhoons. In this study, we employed spectroscopic techniques to investigate the DOM in the eutrophic Zhanjiang Bay before and after Typhoon Ewiniar, aiming to elucidate its origins and decomposition processes and gain insights into the influence of typhoon on DOM decomposition in this eutrophic bay.

2 Materials and methods

2.1 *Typhoon Ewiniar and sampling collection*

Typhoon Ewiniar originated in the central SCS on June 2, 2018, and then slowly moved northward, circling around the coastline of northeastern Hainan Province and the Leizhou Peninsula on June 6, 2018. It subsequently proceeded northeastward, making landfall in Guangdong Province and Hainan Province on June 7, 2018. Ewiniar traveled at an approximate speed of 10 km/h and was characterized by its slow pace, intricate path, and multiple landings. The maximum recorded average wind speed was 23 m/s (Fig. 1). Additionally, because of its slow speed, Typhoon Ewiniar brought a significant amount of rainfall to the western coast of Guangdong Province (Fig. 2).

Zhanjiang Bay is a typical semi-enclosed bay spanning approximately 490 km^2 with water depths ranging from 5 m to 40 m (Peng et al., 2020; Chen et al., 2022; Lao et al., 2022b). It is surrounded by Zhanjiang City, Nansan Island, and Donghai Island (Fig. 1). Seawater in Zhanjiang Bay is primarily influenced by the discharge of freshwater from the Suixi River into the upper bay and the intrusion of high-salinity water from the SCS (Lao et al., 2022b). However, owing to the narrow mouth of the bay (<2 km), there is a slow water exchange between Zhanjiang Bay and the SCS. Because a typhoon passed from June 2nd to 10th, 2018, the sampling conducted on May 12th–14th, 2018 was designated as pre-typhoon sampling. The sampling carried out on June 17th–20th, 2018, was designated as post-typhoon sampling. A total of twenty-six stations were designed in the two cruises, with sampling layers at depths of 0 m, 5 m, 10 m, 15 m, 20 m, 30 m, 40 m as well as a layer located 0.5 m above the bottom. Water temper-

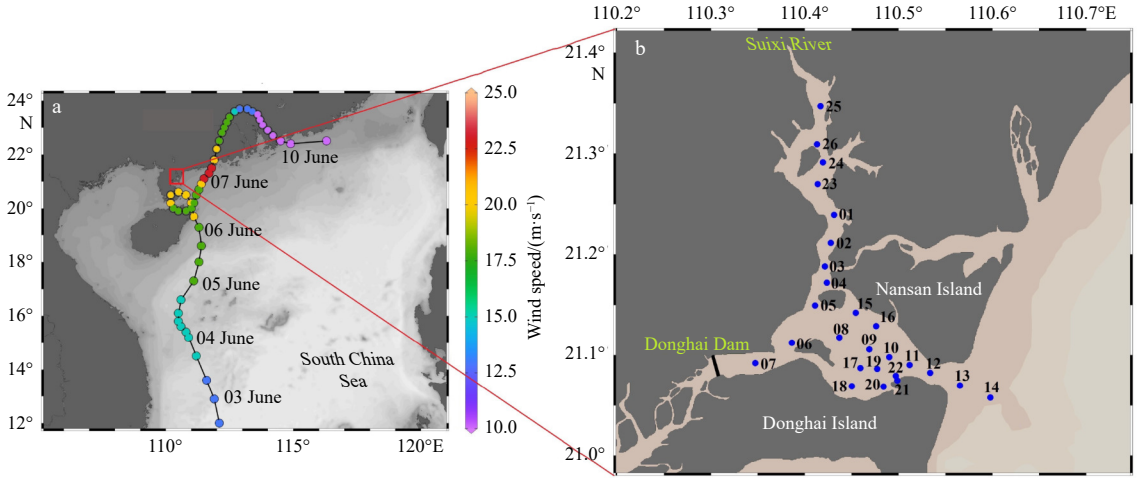

Fig. 1. Map of the passage and intensity (wind speed) of Typhoon Ewiniar (a), and the sampling stations in Zhanjiang Bay (b), northwestern South China Sea, during the pre- and post-typhoon periods.

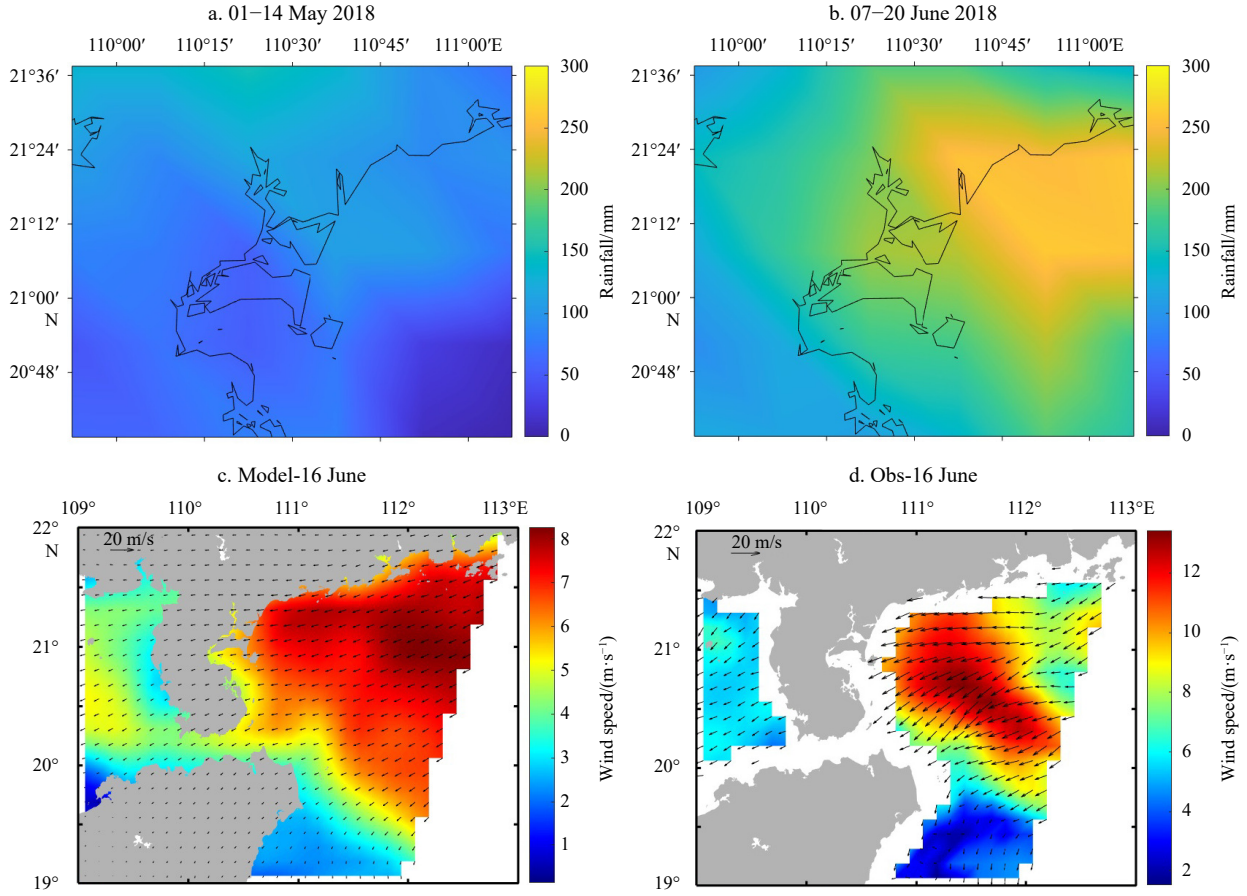

Fig. 2. The rainfall and wind-stress during the Typhoon Ewiniar. a and b are accumulated rainfall before (May 01–14) and during and after (June 07–20) typhoon passage (https://disc.gsfc.nasa.gov/datasets/TRMM_3B42_Daily_7/summary). c is the numerical model results and d is the satellite observations. The daily data of numerical models are obtained from Global Ocean Hourly Reprocessed Sea Surface Wind and Stress from Scatterometer and Model (https://data.marine.copernicus.eu/product/WIND_GLO_PHY_L4_MY_012_006/ description). The daily data of satellite observations are obtained from Global Ocean Daily Gridded Sea Surface Winds from Scatterometer (https://data.marine.copernicus.eu/product/WIND_GLO_WIND_L3_NRT_OBSERVATIONS_012_002/description).

ature and salinity were measured onsite using a CTD (SBE911, Seabird, USA). Dissolved oxygen (DO) was collected during water sampling and preserved by adding manganese chloride and alkaline potassium iodide. 1–2 L of seawater was filtered using a glass fiber membrane (0.7 μm, Whatman GF/F), and the membrane was stored in a refrigerator at –20℃ for subsequent determination of Chl *a*. The water samples were filtered using 0.45 μm acetate membranes and subsequently stored in polyethylene bottles that have been pre-soaked in 30% hydrochloric acid for 24 hours, in the absence of light at low temperature, to facilitate subsequent nutrient and DOM determinations.

2.2 *Measurements of DO, nutrients, Chl a, Chemical oxygen demand*

The DO content was determined using iodometric titration (Grasshoff et al., 1999). The AOU was calculated as the difference between the saturation and observed DO concentrations. The DO saturation (DO%) was determined by dividing the saturated DO concentration by the observed DO concentration. For the extraction of Chl *a* content, a filter membrane was used with 10 mL of 90% acetone, which was determined spectrophotometrically (Lorenzen, 1967). Ammonium (NH_4^+) was determined using the manual indophenol blue method with a UV-Vis spectrophotometer (TU1810), and the other four nutrients (NO_2^-, NO_3^-, PO_4^{3-}, and SiO_3^{2-}) were analyzed using a Skalar San++ continuous analyzer (Netherlands) (Grasshoff et al., 1999). Chemical oxygen demand (COD) measurements were conducted in accordance with Part 4 of the *National Marine Monitoring Code for Seawater Analysis* (GB 17378.4–2007).

2.3 *CDOM analysis*

The absorption spectrum of the CDOM was measured using a UV-visible spectrophotometer (Shimadzu UV-1780, Japan) equipped with a 10 cm quartz test tube. The absorbance (A_λ) was obtained in the wavelength range of 240 nm to 800 nm at intervals of 0.5 nm. Additionally, for quality control purposes, ultrapure water was used as a reference, and every five samples were inserted. The CDOM absorption coefficient (a_λ) was calculated as:

$$a_\lambda = A_\lambda \times 2.303/L, \tag{1}$$

where A is the absorbance of the instrument, λ is the wavelength (nm), and L is the light pathlength (m).

The absorption coefficients at 254 nm (a_{254}) and 325 nm (a_{325}) were used to quantify the CDOM abundance. The log-trans-

formed absorption coefficients were linearly fitted to calculate the spectral slope within the range of 275–295 nm, which can serve as a reliable indicator for assessing the relative molecular weight of DOM (Helms et al., 2008).

2.4 *FDOM analysis and PARAFAC modeling*

An F-7100 fluorescence spectrometer manufactured by Hitachi was used to collect the excitation-emission matrices (EEMs) of the FDOM. EEMs were determined using a four-pass 1 cm quartz cuvette. The excitation (Ex) wavelength ranged from 240 nm to 450 nm in 5 nm increments, whereas the emission (Em) wavelength ranged from 280 nm to 600 nm in 2 nm increments. The excitation and emission slit widths were set to 10 nm and 5 nm, respectively. Raman scattering was eliminated from the sample spectra using Milli-Q water as reference. Rayleigh scattering was removed by replacing the EEM data in two regions (Em ⩽ Ex + 20 nm; Em ⩾ 2Ex – 10 nm) with zero. The fluorescence intensity was normalized to Raman units (RU) using the Raman correction procedure reported by Lawaetz and Stedmon (2009). An absorptivity-based method was employed to correct the internal filtering effects. The parallel factor analysis method (PARAFAC) in MATLAB 2016a and DOM Fluor toolbox were used to decompose all EEMs into a set of fluorescence components. The humification index (HIX), which represents the ratio of the integral area of Em at 254 nm from 435–480 nm to that between 300–345 nm for Ex, was utilized as an indicator to assess the degree of DOM humification (Zsolnay et al., 1999). Higher HIX values indicated a higher degree of humification. The biogenic index (BIX) was calculated as the ratio of the fluorescence intensity of Em at 380 nm and 430 nm to that of Ex at 310 nm (Huguet et al., 2009). Higher BIX values indicated an increasing contribution of freshly produced DOM to aquatic ecosystems. The FI, which is the ratio of the fluorescence intensities of Em at 450 nm and 500 nm to that of Ex at 370 nm, can be used to trace the source of DOM (Stedmon and Bro, 2008). When the FI value is >1.9, the DOM is generally sourced from a biological origin, whereas when the FI value is <1.4, the DOM generally originates from a terrestrial origin.

The PARAFAC model was used to analyze the three fluorescence components (Fig. S1). C1 exhibited an excitation wavelength of 250 nm and an emission wavelength of 406 nm, similar to the previously reported A peak observed in terrestrial humic-like components (Coble, 1996, 2007). C2 included two excitation wavelengths at 265 nm and 365 nm, along with an emission wavelength of 442 nm, covering humic-like A and C peaks (Coble, 1996, 2007). C3 exhibited an excitation wavelength of 275 nm and an emission wavelength of 326 nm, similar to the previously reported T peak associated with the protein-like fluorescent component (Coble, 1996, 2007).

2.5 *Two end-member mixing model*

A two-end model was employed to calculate the addition and removal of nutrients and DOM to investigate their biogeochemical behavior in Zhanjiang Bay. The surface layer of Station 25 was used as the low-salinity endmember before the typhoon; however, there were no available FDOM component data for the same layer after the typhoon. To maintain consistency in our calculations, we selected the surface layer at Station 26 as the low-salinity endmember after the typhoon. The bottom layer at Station 14 remained unchanged and continued to serve as a high-salinity endmember both before and after the typhoon. The two-end model equations are as follows:

$$f_{up} + f_{ou} = 1, \tag{2}$$

$$f_{up}\mathrm{Sal}_{up} + f_{ou}\mathrm{Sal}_{ou} = \mathrm{Sal}, \tag{3}$$

where f_{up} and f_{ou} represent the proportions of the low-salinity endmembers in the upper bay and high-salinity endmembers in the outer bay, respectively, for each sample. Sal_{up} and Sal_{ou} represent the salinity of the low-salinity and high-salinity endmembers, respectively, whereas Sal represents the salinity of the sample. By subtracting the conservative theoretical values from the actual values of nutrients and DOM, one can obtain the ΔN, which represents the conservative change in nutrient and DOM based on measured data:

$$\Delta N = N - f_{up}N_{up} - f_{ou}N_{ou}, \tag{4}$$

where, N refers to nutrients and DOM, and a positive ΔN represents the net addition of nutrients and DOM during the water mass mixing process, while a negative ΔN represents the net removal of nutrients and DOM. The end number values before and after the typhoon are listed in Tables S1 and S2, respectively.

2.6 *The eutrophication index method*

The eutrophication index (EI) is calculated as follows (Huang et al., 2022; Ke et al., 2022):

$$\mathrm{EI} = C_{\mathrm{COD}} \times C_{\mathrm{DIN}} \times C_{\mathrm{DIP}}/0.045, \tag{5}$$

where C_{COD}, C_{DIN}, and C_{DIP} are measured concentrations of COD, DIN, and PO_4^{3-} (unit: mg/L), respectively. Water is considered non-eutrophic if EI is less than 1, and slightly eutrophic if 1 < EI < 2. The water body was considered moderately eutrophic when 2 < EI < 5. Water bodies can be categorized as highly eutrophic when 5 < EI < 15. If the value of EI exceeded 15, the water body was regarded as severely eutrophic (Huang et al., 2022; Ke et al., 2022; Andersen et al., 2017; Lao et al., 2021).

2.7 *Statistical analysis*

Statistical analysis was performed using SPSS 22.0, and the Student's *t*-test was used to compare the differences between the two groups of parameters.

3 Results

3.1 *Distribution of physiochemical parameters during pre-typhoon and post-typhoon*

The distribution figures of the physiochemical parameters on the surface are presented here because of the similarity in distribution between the surface and bottom for all parameters, whereas those at the bottom are provided in the Figs S2–S5. The distributions of temperature, salinity in the Zhanjiang Bay during the pre- and post-typhoon periods are shown in Fig. 3. Lower temperatures were consistently observed at the mouth of the bay during both the periods. However, the water column temperature during the post-typhoon [(30.06 ± 0.80)℃] was significantly higher than that during the pre-typhoon [(28.08 ± 0.58)℃] (*t*-test, $p < 0.001$). Salinity gradually increased from the upper bay to the outer bay during both periods. In addition, there was a decrease in salinity in the upper bay following typhoon activity, suggesting an influx of freshwater. Nevertheless, the water column salinity during the post-typhoon (28.09 ± 3.05) was higher compared to the salinity during the pre-typhoon (27.79 ± 1.62) (Table 3).

The distributions of DO concentrations during the pre- and

post-typhoon periods are shown in Fig. 3. Higher DO concentrations were observed in the middle of the bay during the pre-typhoon period, whereas after the typhoon, elevated DO levels were found near the mouth of the bay, with an extremely high value recorded at Station 7. Overall, the average concentration of DO in the water column before the typhoon [(6.74 ± 0.66) mg/L] exceeded that after the typhoon [(5.78 ± 0.69) mg/L]. The DO% and DO distributions were similar during the pre- and post-typhoon periods, but the opposite pattern was observed in the distribution of the AOU (Fig. 3).

The water column Chl *a* concentrations [(11.50±6.39) mg/L] were significantly higher during the pre-typhoon compared to the post-typhoon [(7.43±7.30) mg/L] (*t*-test, $p < 0.001$). However, higher Chl *a* concentrations were observed in the upper bay (stations 1–5) during the pre-typhoon period, whereas anomalously high Chl *a* concentrations were observed at stations 7 and 9 during the post-typhoon period. Our previous study demonstrated the nutrient parameters in Zhanjiang Bay during the same cruise in June 2018 (He et al., 2023). The distribution of nutrients during the pre- and post-typhoon periods is shown in Fig. 4. Nutrient distribution was primarily characterized by a gradual decrease from the upper bay to its mouth, indicating significant in-

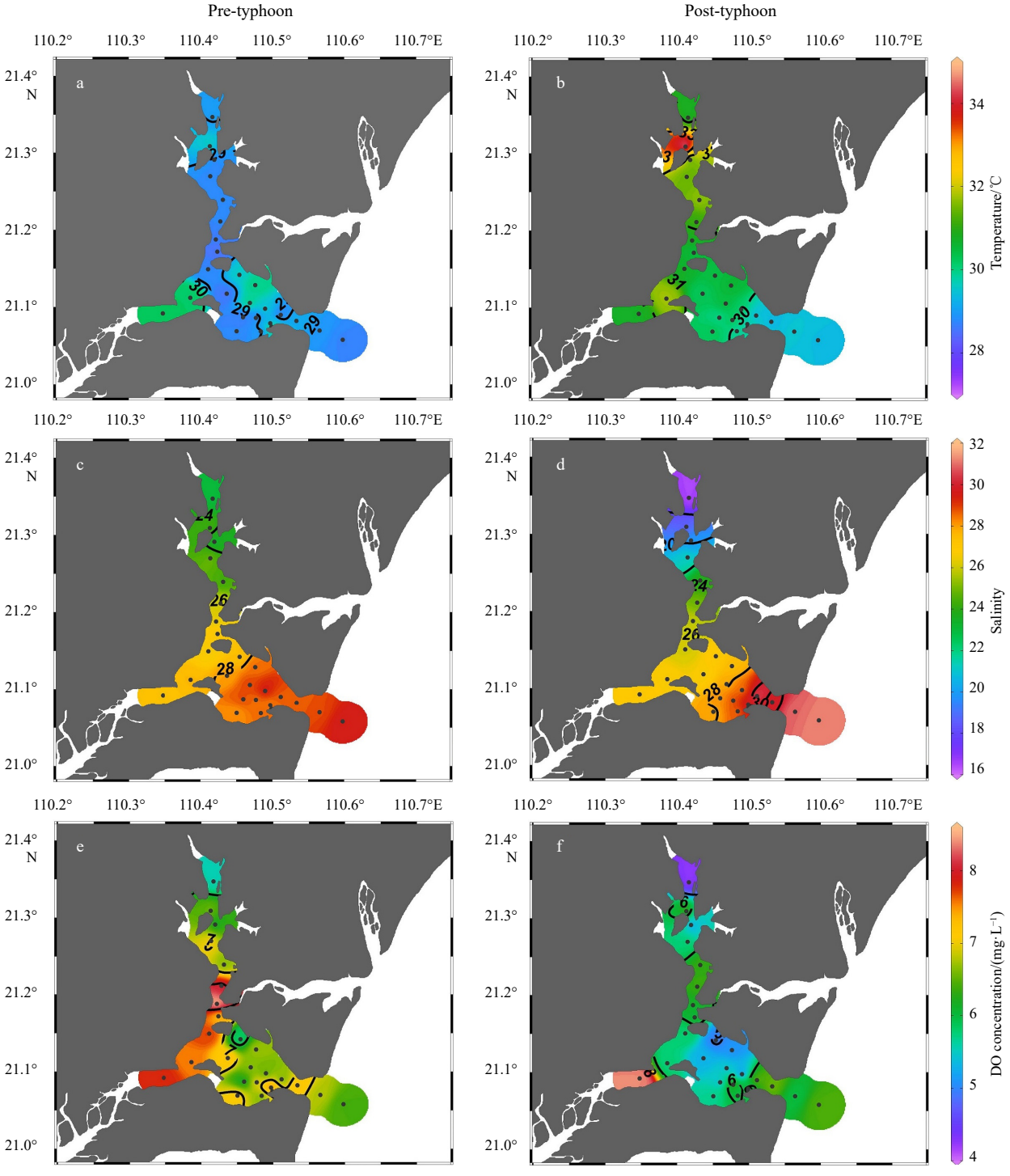

Fig. 3.

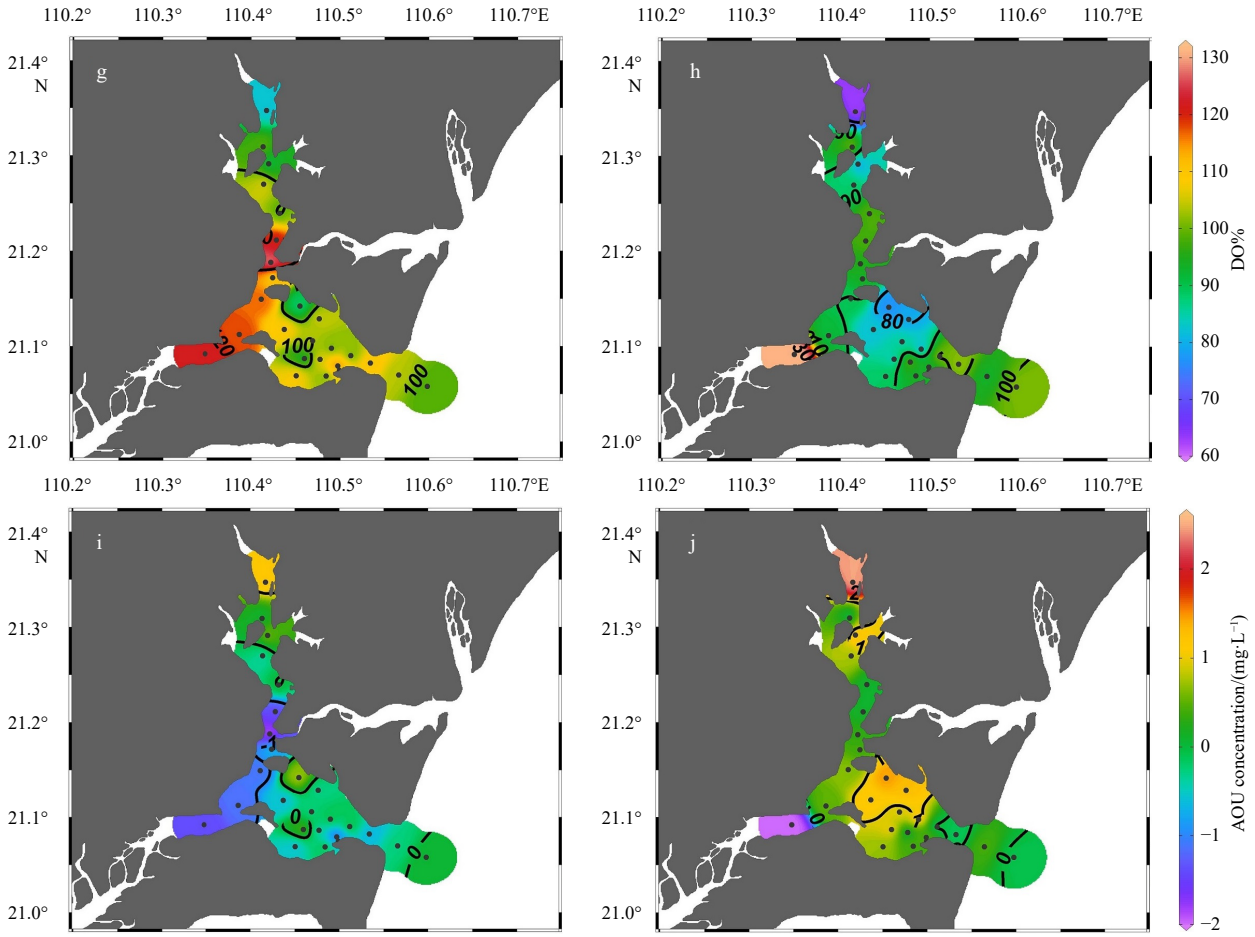

Fig. 3. Surface distribution of temperature, salinity, DO, DO% and AOU in the Zhanjiang Bay during pre- and post-typhoon periods.

put from land. The water column DIN concentrations [NH_4^+ + NO_2^- + NO_3^-, (27.83 ± 17.60) μmol/L] and PO_4^{3-} [(2.82 ± 1.48) μmol/L] during the pre-typhoon were higher than those during the post-typhoon [DIN: (15.15 ± 11.16) μmol/L; PO_4^{3-}: (2.67 ± 1.65) μmol/L]. However, the water column SiO_3^{2-} concentration [(9.40 ± 13.27) μmol/L] during the pre-typhoon was significantly lower than that during the post-typhoon [(21 .96 ± 11 .86) μmol/L] (*t*-test, $p < 0.001$).

3.2 *Distribution of CDOM, $S_{275-295}$, FDOM, FI, HIX, and BIX in Zhanjiang Bay pre- and post-typhoon*

The distribution characteristics of the CDOM (a_{254} and a_{325}) are shown in Fig. 5. Both a_{254} and a_{325} gradually decreased from the upper bay to the mouth during the pre- and post-typhoon periods. However, the levels of water column a_{254} [(2.84 ± 1.35) m^{-1}] and a_{325} [(0.84 ± 0.52) m^{-1}] during the pre-typhoon were higher than those during the post-typhoon [a_{254}: (1.88 ±

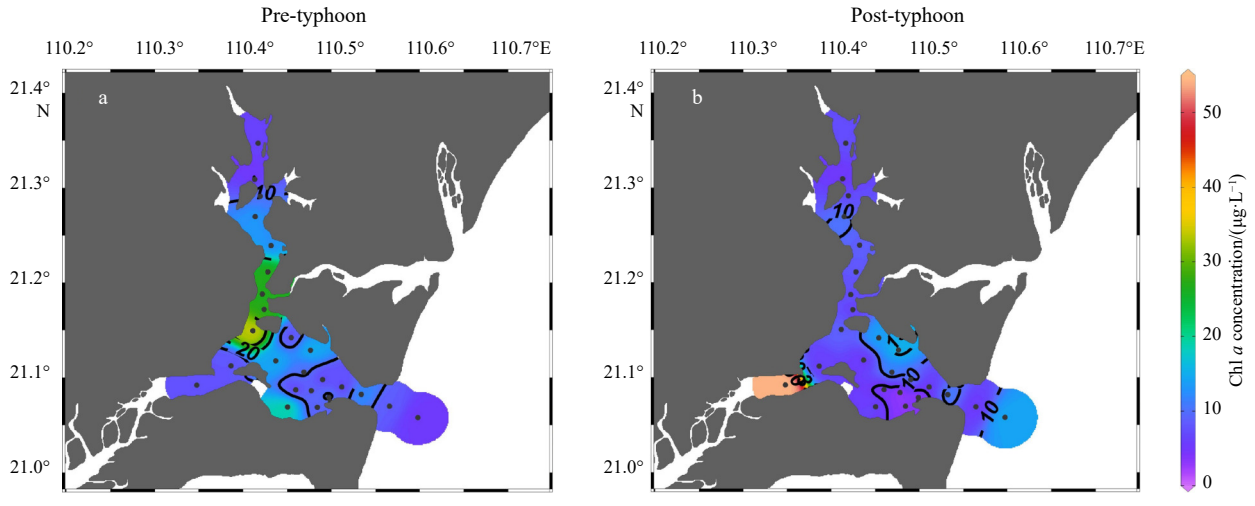

Fig. 4.

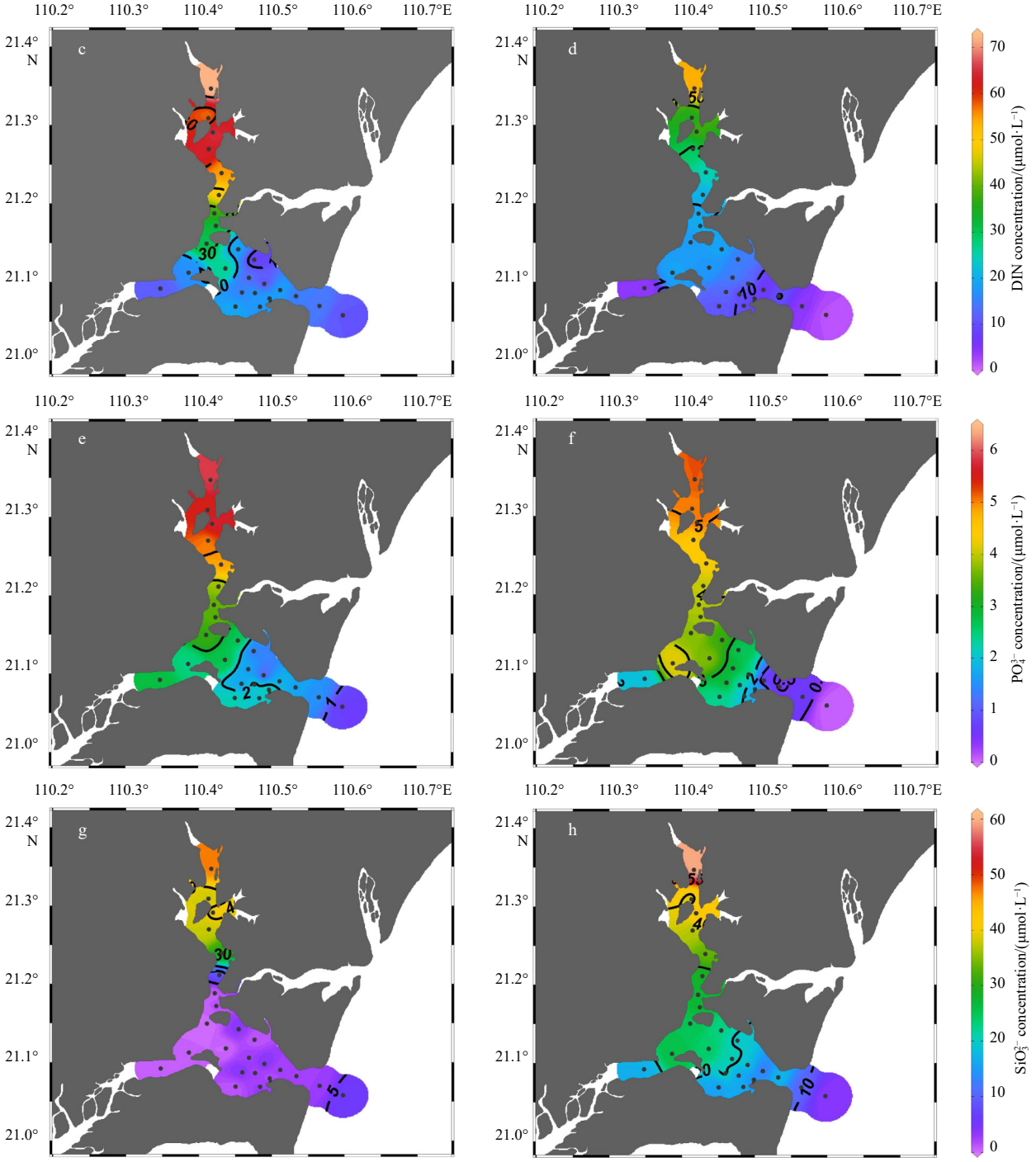

Fig. 4. Surface distribution of Chl *a*, DIN ($NH_4^+ + NO_2^- + NO_3^-$), PO_4^{3-}, and SiO_3^{2-} in the Zhanjiang Bay during pre- and post-typhoon periods.

0.7) m^{-1} and a_{325}: (0.56 ± 0.27) m^{-1}]. $S_{275-295}$ gradually increased from the top of the bay to its mouth, and the pre-typhoon water column $S_{275-295}$ [(20.41 ± 1.82) μm^{-1}] was slightly higher than that during the post-typhoon [(19.74 ± 1.95) μm^{-1}].

The distributions of C1, C2, and C3 after the typhoon were similar to those of the CDOM, which gradually decreased from the top to the mouth of Zhanjiang Bay (Fig. 6). In addition, water column C1 [(20.59 ± 10.29) × 10^{-2} RU], C2 [(7.50 ± 4.04) × 10^{-2} RU], and C3 [(10.27 ± 2.76) × 10^{-2} RU)] were higher during the pre-typhoon than post-typhoon [(C1: (14.43 ± 6.20) × 10^{-2} RU; C2: (5.47 ± 2.53) × 10^{-2} RU; C3: (6.26 ± 1.59) × 10^{-2} RU]. The HIX gradually decreased from the upper bay to its mouth, whereas the BIX gradually increased along this stretch (Fig. 6). The FI fluctuated throughout the bay, and there was little difference in the FI values between the pre- and post-typhoon periods (Table S3). The HIX was lower during the pre-typhoon period than during the post-typhoon period, and the BIX was higher during the pre-typhoon period than during the post-typhoon period.

4 Discussions

4.1 *High nutrient inputs enhance the decomposition of DOM in Zhanjiang Bay during pre-typhoon.*

The levels of CDOM and FDOM gradually decreased seaward,

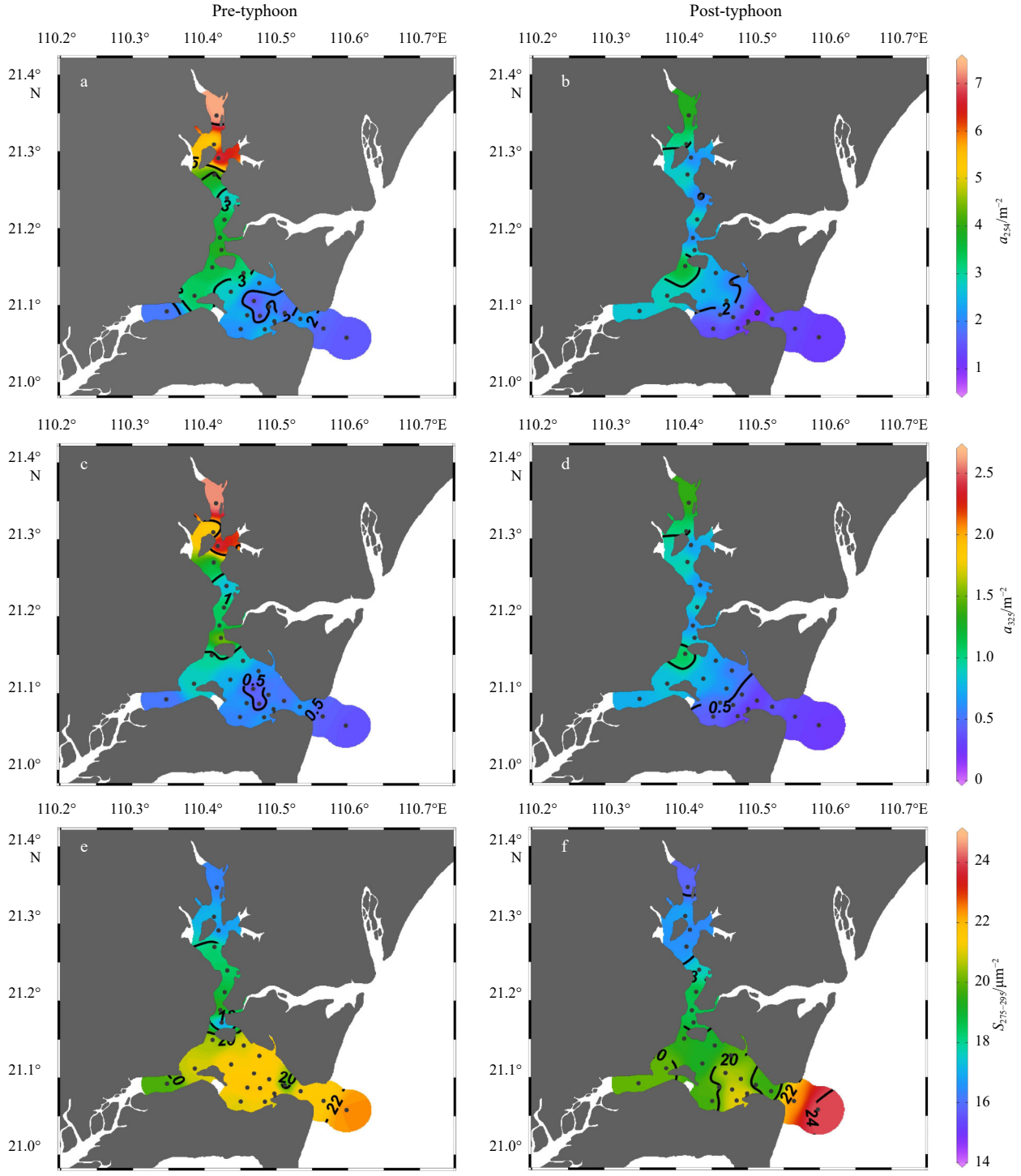

Fig. 5. Surface distribution of a_{254}, a_{325}, and $S_{275–295}$ in the Zhanjiang Bay during pre- and post-typhoon periods.

while $S_{275–295}$ showed the opposite trend (Figs 5 and 6), indicating that DOM was primarily influenced by terrestrial origins during the pre-typhoon period. The significant correlation between CDOM and FDOM ($p < 0.01$) suggested a similar origin for these components. The FDOM was composed of three components, C1, C2, and C3, accounting for 52.5%, 18.9%, and 28.6%, respectively, which were mainly humus-like components. A significant correlation was observed between Chl *a* and the protein-like C3 (Fig. S6a, $p < 0.05$, $n = 97$), suggesting that biological activities influenced the source of C3 (Chiranjeevulu et al., 2014; Letourneau and Medeiros, 2019; Bowen et al., 2020).

In addition, negative Δa_{254} [(−1.33 ± 0.70) m^{-1})], Δa_{325} [(−0.51 ± 0.27) m^{-1}], ΔC1 [(−8.09 ± 4.88) × 10^{-2} RU)], ΔC2 [(−3.73 ± 1.91) × 10^{-2} RU)], and ΔC3 [(−1.38 ± 1.91 × 10^{-2} RU)] were observed in the bay during the pre-typhoon period, indicating a removal of DOM in this time (Fig. 7). There are two main reasons for the removal of DOM from marine environments: photodecomposition and biological decomposition (Helms et al., 2008; Hansen et al., 2016; Catalá et al., 2016). Assuming that the removal of DOM in Zhanjiang Bay is due to photodecomposition, there should be a

gradual increase in ΔDOM from the sea surface to the bottom (indicating decreased removal) and a corresponding decrease in $S_{275-295}$ (indicating increased molecular weight). However, an irregular distribution of ΔDOM and $S_{275-295}$ can be observed along the Zhanjiang Bay transect during the pre-typhoon (Fig. 8), which suggests that photodecomposition is not the primary responsible for DOM removal. Thus, we believe that biological decomposition is the primary factor contributing to DOM removal. Despite the DO in Zhanjiang Bay was close to saturation before the typhoon [with a DO% of 102.30% ± 10.30% and an AOU of (−0.15 ± 0.68) mg/L], the high Chl *a* concentrations [(11.50 ± 6.39) μg/L] suggested abundant nutrients that promoted phytoplankton growth and photosynthesis, which can compensate for any oxygen consumed by DOM decomposition and maintain an oxygen-saturated state.

Previous studies have shown that inputs of N and P from terrestrial origins can decrease the C/N and C/P ratios, thereby promoting the microbial decomposition of labile DOC (Zweifel et al., 1993; Yuan et al., 2010; Jiao et al., 2011, 2018). This process leads to a significant reduction in carbon storage in the ocean (Jiao et al., 2011, 2018). High nutrient levels were also observed in the bay during the pre-typhoon period (Table S4). Owing to the rap-

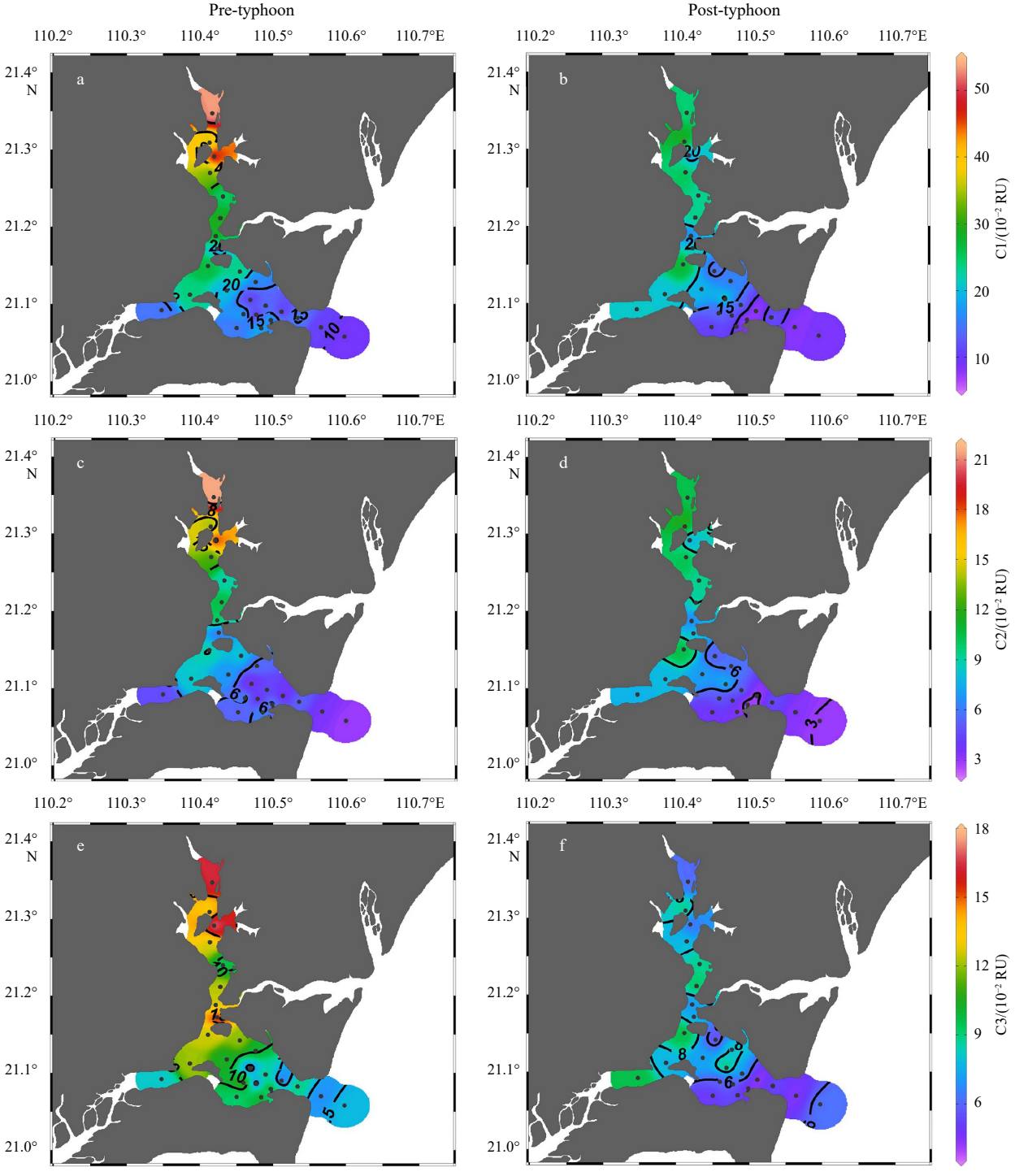

Fig. 6.

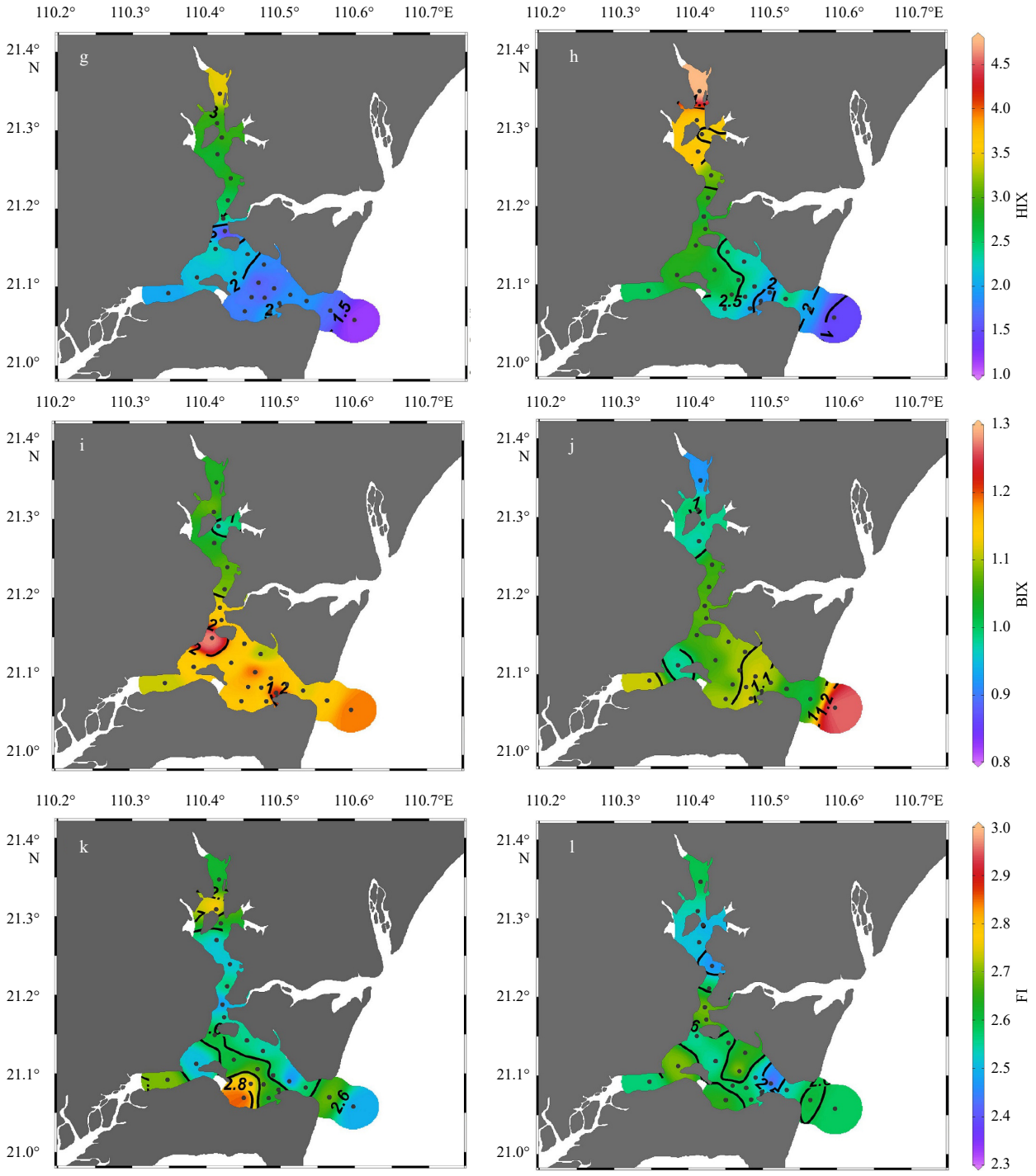

Fig. 6. Surface and bottom distribution of C1, C2, C3, HIX, BIX and FI in Zhanjiang Bay during pre- and post-typhoon periods.

id economic and population growth in recent years, Zhanjiang, an industrial city, has experienced a significant influx of sewage into the bay (Chen et al., 2022; He et al., 2023; Lao et al., 2023d). N and P inputs play a significant role in the eutrophication process in Zhanjiang Bay (He et al., 2023). The eutrophication index was calculated using the EI. The EI ranged from 0.1 to 82.8 with a mean value of 14.9 ± 18.9 (Table S4), indicating that Zhanjiang Bay was currently classified as high levels of eutrophication. Therefore, the input of N and P from Zhanjiang Bay before the typhoon promoted eutrophication in the water column, which may have resulted in lower C/N and C/P ratios. This can stimulate DOC bioactivity, thereby promoting the microbial decomposition of DOM (Zweifel et al., 1993; Yuan et al., 2010; Jiao et al., 2011, 2018). This finding is consistent with previous studies that indicated nearshore waters characterized by eutrophication act as sources of CO_2 rather than sinks in the Zhujiang (Pearl) River Estuary (Yuan et al., 2010). Therefore, the high nutrient inputs in Zhanjiang Bay could have enhanced the intense DOM decomposition during the pre-typhoon period.

4.2 *The decomposition of organic matter shifted from DOM to particulate organic matter (POM) after the typhoon*

Previous studies have indicated that the Ekman transport, or the input of runoff after a typhoon, results in a significant amount

of nutrients (Lao et al., 2023b, 2023d), thereby promoting phytoplankton growth (Zhao et al., 2009, 2015; Qiu et al., 2019; Lu et al., 2022a). However, our results demonstrate that Chl *a* levels decreased after the typhoon, which is consistent with recent research conducted in Zhanjiang Bay (Zhou et al., 2021). They suggested that the stirring caused by the typhoon resulted in the deterioration of seawater quality, which was unfavorable for the growth of phytoplankton (Lao et al., 2023d; Zhou et al., 2021). It is widely accepted that rainfall after a typhoon brings a greater amount of DOM from terrestrial origins, and the levels of DOM during this period are also significantly higher than those before the typhoon (Hoge and Lyon, 2002; Conmy et al., 2009; Letourneau and Medeiros, 2019). However, terrestrial inputs did not significantly contribute to DOM in Zhanjiang Bay during the post-typhoon period. CDOM and FDOM exhibited a significant decrease during the post-typhoon period compared to the pre-typhoon levels (*t*-test, $p < 0.001$). Despite receiving greater rainfall after the typhoon (>250 mm) than before the typhoon (~150 mm) in the area around Zhanjiang Bay (Fig. 2), there was a slight increase in salinity during the post-typhoon period in Zhanjiang Bay. This phenomenon indicated that high-salinity water from the outer bay intruded into Zhanjiang Bay after the typhoon (Lao et al., 2022b, 2023d). As shown in Figs 2c and 2d, this shift in sea-surface winds in the northwestern SCS contributed to the influx of high-salinity seawater from the SCS into the bay. Previous studies have found that the intrusion of high-salinity seawater from outer Zhanjiang Bay increases substantially under the external forces of typhoons (Lao et al., 2023d). These phenomena suggest that the decrease in DOM in Zhanjiang Bay after the typhoon may be attributed to the dilution caused by seawater intrusion from the outer bay. The correlation between Chl *a* and protein-like C3 (Fig. S6b, $p < 0.05$, $n = 94$) suggests a strong association between the origin of the C3 component and the biological activity (Chiranjeevulu et al., 2014; Letourneau and Medeiros, 2019; Bowen et al., 2020). The percentages of humus-like C1 (54.3%) and C2 (20.4%) were slightly higher during the post-typhoon period than during the pre-typhoon period, whereas that of protein-like C3 (25.4%) was lower than that before the typhoon. The decrease in Chl *a* during the post-typhoon period may be the main reason for the decline in protein-like components.

Notably, there were significant net additions of CDOM [Δa_{254}: (0.24 ± 0.52) m^{-1}, Δa_{325}: (0.07 ± 0.16)m^{-1}] and FDOM [ΔC1: (1.39 ± 6.21) × 10^{-2} RU, ΔC2: (0.39 ± 2.45) × 10^{-2} RU, ΔC3: (0.46 ± 2.04) ×

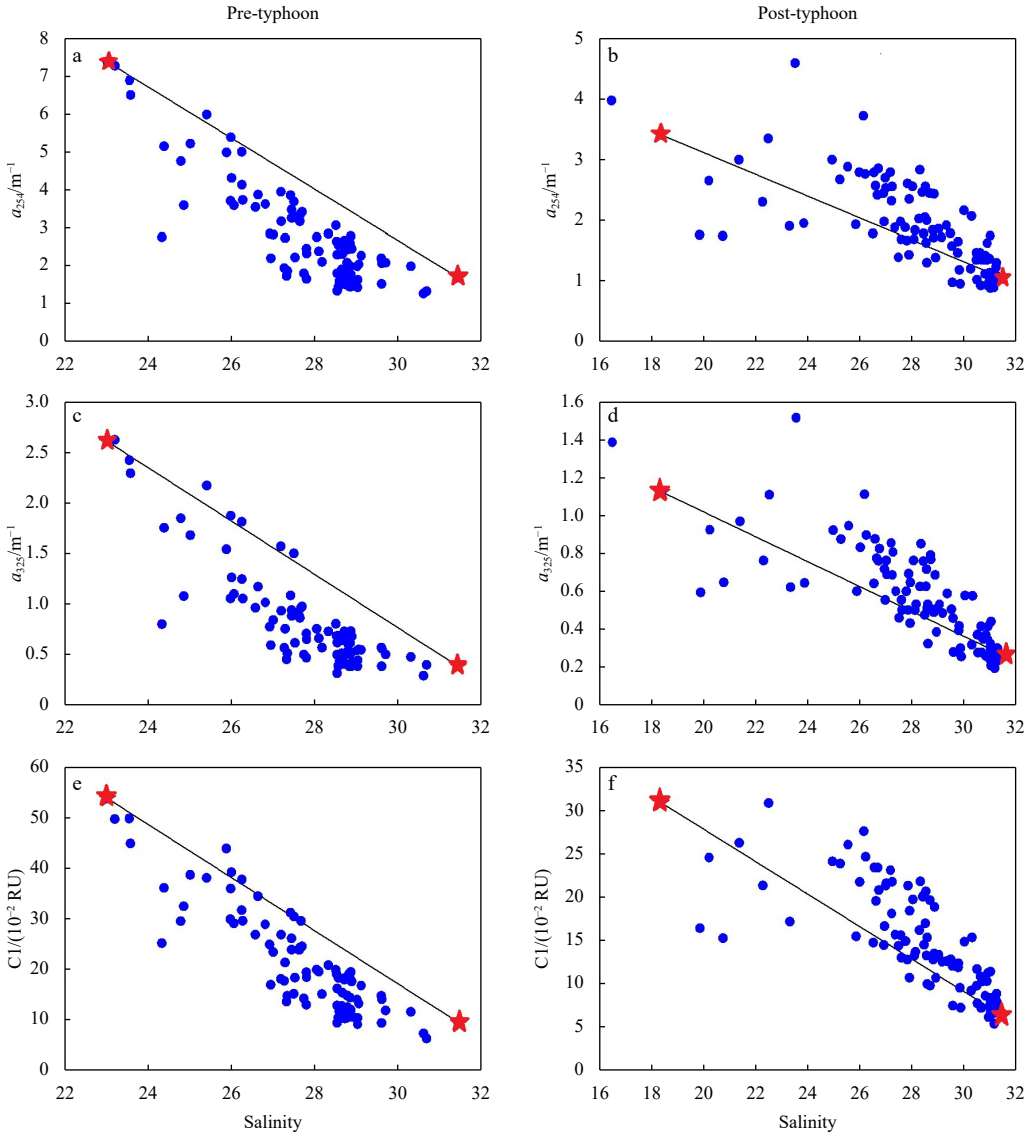

Fig. 7.

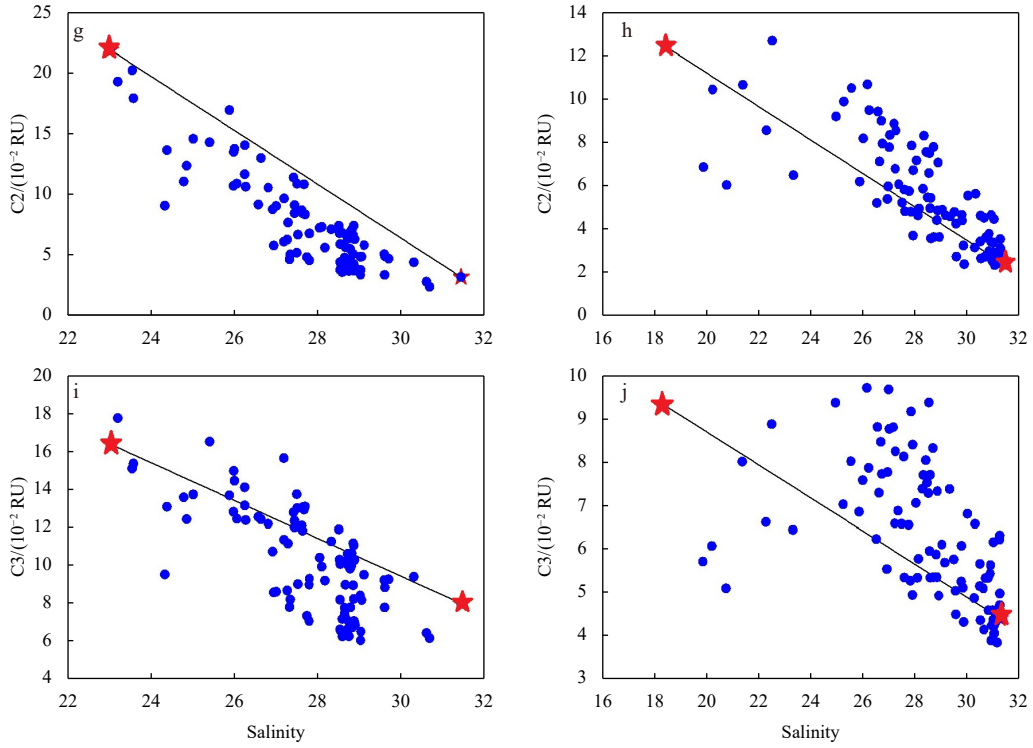

Fig. 7. Variations of a_{254} (m^{-1}) (a, b), a_{325} (m^{-1}) (c, d), C1 (10^{-2} RU) (e, f), C2 (10^{-2} RU) (g, h), C3 (10^{-2} RU) (i, j) along with salinity in the water of Zhanjiang Bay during the pre-typhoon and post-typhoon. The red stars denote the low-salinity and high-salinity end-members used in this study.

10^{-2} RU] in Zhanjiang Bay during the post-typhoon (Fig. 9, Table S5). This suggests that, in contrast to the pre-typhoon period, there was no decomposition of DOM. Instead, it is likely that other origins or processes supplemented the DOM in the bay. Nutrient concentrations (DIN and PO_4^{3-}) decreased significantly after the typhoon (Fig. 4). Additionally, the EI indicated a reduction of 6.56 ± 11.55 (Table S4). The intrusion of seawater from the outer bay can dilute the DOM and nutrient concentrations, which may be responsible for the decrease in these parameters after the typhoon. A reduction in nutrient concentrations promotes the immobilization of DOC and storage of microbial carbon (Carlson et al., 2002; Gasol et al., 2009; Jiao et al., 2011). Therefore, the decrease in nutrient levels induced by typhoons resulted in a reduction in the microbial decomposition of DOM.

In the marine environment, in addition to external inputs, DOM is primarily contributed by phytoplankton release, OM decomposition, and particulate matter desorption (Guo et al., 2007, 2014; Sun et al., 2022; Hu et al., 2022). There was no correlation between Δa_{254}, Δa_{325}, ΔC1, ΔC2, ΔC3 and Chl *a* ($p > 0.05$) after the typhoon, suggesting that the addition of DOM is not primarily caused by phytoplankton production (Guo et al., 2011; Lu et al., 2023). We speculate that the decomposition of POM and desorption of particulate matter may have contributed to the addition of DOM. The presence of a positive AOU concentration indicated oxygen depletion after a typhoon. Oxygen depletion in the water column results primarily from the oxidation of inorganic substances, biological respiration, and OM decomposition (Chen, 2009). The oxidation of inorganic matter consumes a lower amount of oxygen than biological respiration and OM decomposition; therefore, the oxidation of inorganic matter was considered negligible in this study (Chen, 2009; Lu et al., 2022a). Although a short-term increase in Chl *a* may occur after typhoons (Chen et al., 2023), the stirring caused by typhoons results in the deterioration of the water environment in Zhanjiang Bay, which inhibits phytoplankton growth (Zhou et al., 2021). This is supported by the observed decrease in Chl *a* levels after the typhoon. Therefore, the primary cause of oxygen depletion in Zhanjiang Bay after the typhoon is the decomposition of OM. Consequently, the significant decrease in Chl *a* after the typhoon suggests a preference for decomposing fresh POM (Zhou et al., 2021; Lu et al., 2022a; Lao et al., 2023c). This conclusion is consistent with the above discussion regarding the addition of DOM through the decomposition of POM (Wang et al., 2021a; Qu et al., 2022; Chen et al., 2022; Lu et al., 2023). The net addition of nutrients to Zhanjiang Bay after the typhoon provides further evidence to support this conclusion (Fig. S7). Although the desorption of particulate matter is commonly observed in highly turbid estuaries such as the Changjiang River Estuary (Guo et al., 2014; Sun et al., 2022), we cannot rule out the influence of particulate matter desorption on DOM addition. However, further studies are required to clarify this issue.

4.3 *Implications of the characteristics of OM decomposition*

In eutrophic estuaries or bays, DOM decomposition is often considered a source of CO_2 rather than a sink because of microbial-mediated decomposition, which converts organic carbon into CO_2 (Zweifel et al., 1993; Yuan et al., 2010; Jiao et al., 2011, 2018). In this study, we found that microbial decomposition of DOM was enhanced during the pre-typhoon period due to a substantial influx of N and P inputs. However, contrary to expectations, the typhoons did not increase DOM decomposition. Instead, it may induce a significant shift from DOM to POM decomposition, providing a deeper understanding of the carbon cycle in nearshore areas (Fig. 9). This phenomenon is related to a short-term increase in Chl *a* after typhoons (Chen et al., 2023). In our study, an increase in apparent oxygen utilization, a decrease in DO sat-

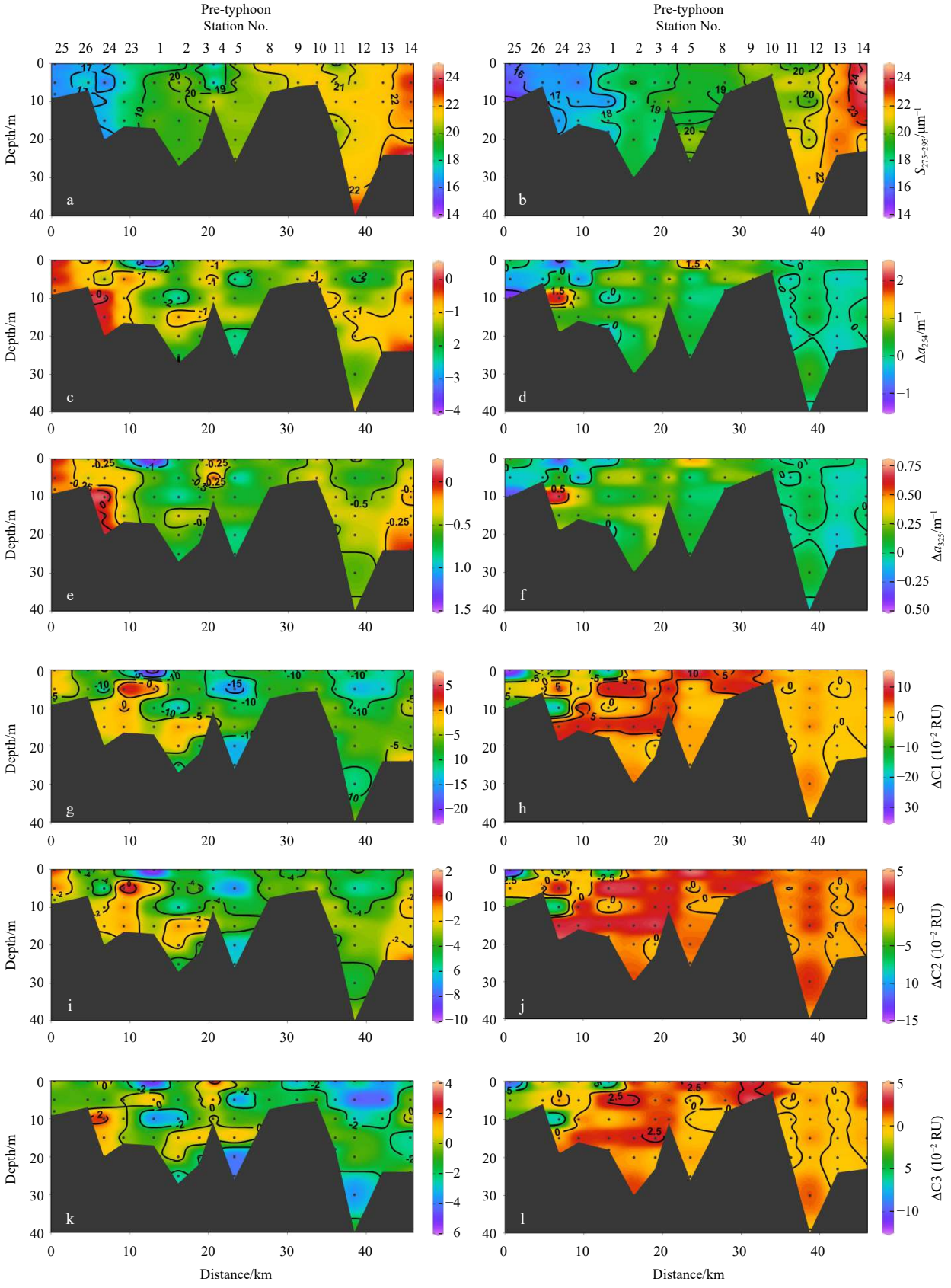

Fig. 8. Transect distribution of $S_{275-295}$, Δa_{254}, Δa_{325}, ΔC1, ΔC2, and ΔC3 in the Zhanjiang Bay during pre- and post-typhoon periods.

uration, and a reduced level of Chl *a* indicated that POM decomposition was enhanced in Zhanjiang Bay after the typhoon. Thus, the net addition of DOM occurred in Zhanjiang Bay after the typhoon. Nonetheless, we believe that OM may undergo different types and degrees of decomposition under various typhoon paths, intensities, and moving speeds (Chen et al., 2023). In addi-

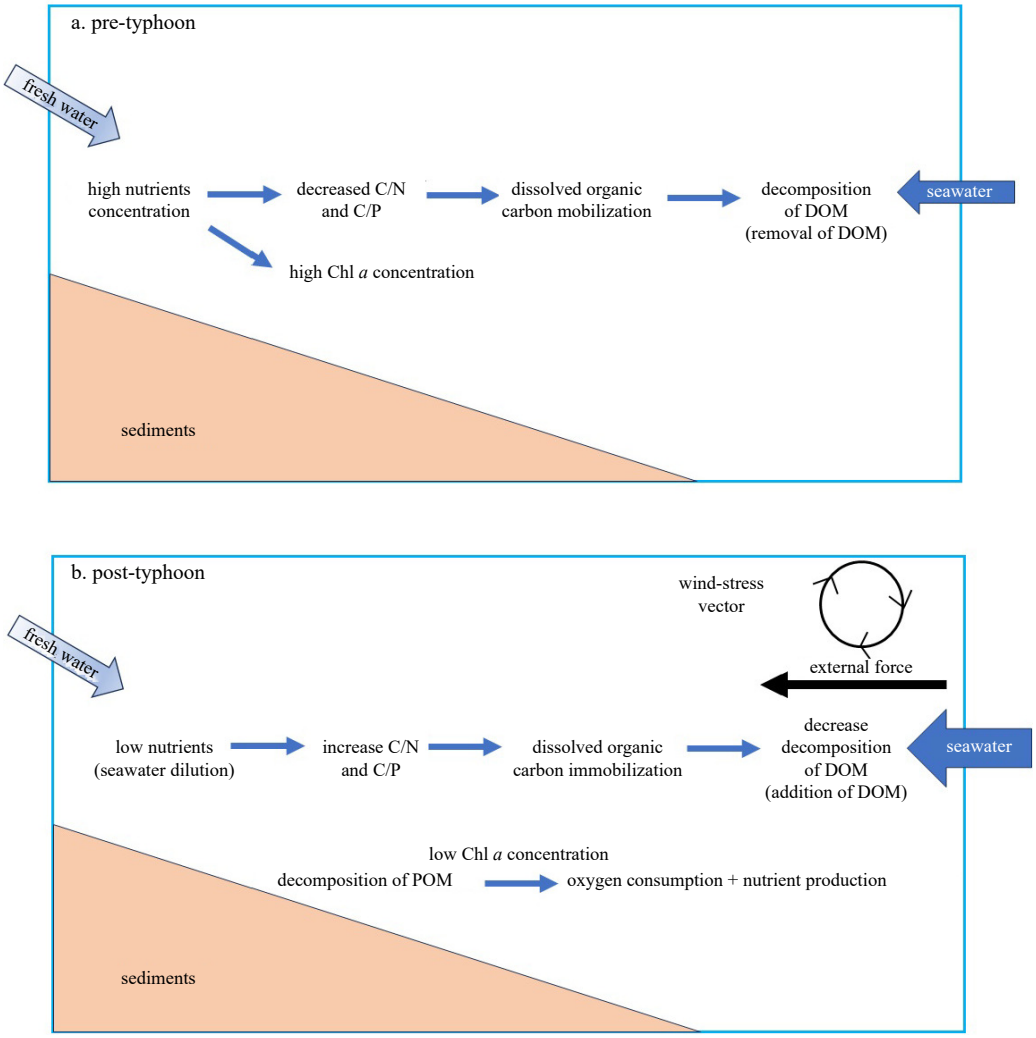

Fig. 9. Simplified schematic sketch summarizing the decomposition of OM in Zhanjiang Bay, northwestern South China Sea, during the pre- and post-typhoon periods.

tion, the intensity of typhoons has significantly increased under global warming (Balaguru et al., 2016; Chen et al., 2023), and it is necessary to consider the types and degrees of OM decomposition (as a carbon source) following typhoons in the future.

5 Conclusions

In this study, spectroscopic techniques were used to investigate the origin and decomposition of DOM before and after Typhoon Ewiniar in Zhanjiang Bay, in the northwestern SCS. The two-end-member mixing model demonstrated the removal of DOM before the typhoon and the addition of DOM after the typhoon. High nutrient input resulted in intense microbial decomposition of DOM during the pre-typhoon period. However, the net addition of DOM in Zhanjiang Bay may be attributed to POM decomposition and desorption of particulate matter during the post-typhoon period. The intrusion of external seawater dilutes the nutrient levels in Zhanjiang Bay, thus diminishing the impact of microbial decomposition on DOM. However, an increase in the AOU, a decrease in the DO saturation value and the reduced Chl *a* concentrations indicated that intense OM decomposition still occurred and OM decomposition shifted to POM decomposition in Zhanjiang Bay during the post-typhoon period. Overall, this study provided new insights into the impact of typhoons on biogeochemistry.

References

Andersen J H, Carstensen J, Conley D J, et al. 2017. Long-term temporal and spatial trends in eutrophication status of the Baltic Sea. Biological Reviews, 92(1): 135–149, doi: 10.1111/brv.12221

Asmala E, Haraguchi L, Markager S, et al. 2018. Eutrophication leads to accumulation of recalcitrant autochthonous organic matter in coastal environment. Global Biogeochemical Cycles, 32(11): 1673–1687, doi: 10.1029/2017GB005848

Balaguru K, Foltz G R, Leung L R, et al. 2016. Global warming-induced upper-ocean freshening and the intensification of super typhoons. Nature Communications, 7: 13670, doi: 10.1038/ncomms13670

Bowen J C, Kaplan L A, Cory R M. 2020. Photodegradation disproportionately impacts biodegradation of semi-labile DOM in streams. Limnology and Oceanography, 65(1): 13–26, doi: 10.1002/lno.11244

Carlson C A, Giovannoni S J, Hansell D A, et al. 2002. Effect of nutrient amendments on bacterioplankton production, community structure, and DOC utilization in the northwestern Sargasso Sea. Aquatic Microbial Ecology, 30(1): 19–36, doi: 10.3354/ame030019

Catalá T S, Álvarez-Salgado X A, Otero J, et al. 2016. Drivers of fluorescent dissolved organic matter in the global epipelagic ocean. Limnology and Oceanography, 61(3): 1101–1119, doi: 10.1002/lno.10281

Chen Min. 2009. Chemical Oceanography (in Chinese). Beijing: China Ocean Press, 33–59

Chen Fajin, Huang Chao, Lao Qibin, et al. 2021. Typhoon control of precipitation dual isotopes in southern China and its palaeoenvironmental implications. Journal of Geophysical Research: Atmospheres, 126(14): e2020JD034336, doi: 10.1029/2020JD034336

Chen Zhiqiang, Li Yan, Pan Jianming. 2004. Distributions of colored dissolved organic matter and dissolved organic carbon in the Pearl River Estuary, China. Continental Shelf Research, 24(16): 1845–1856, doi: 10.1016/j.csr.2004.06.011

Chen Fajin, Lao Qibin, Liu Mengyang, et al. 2022. Impact of intensive mariculture activities on microplastic pollution in a typical semi-enclosed bay: Zhanjiang bay. Marine Pollution Bulletin, 176: 113402, doi: 10.1016/j.marpolbul.2022.113402

Chen Fajin, Lao Qibin, Lu Xuan, et al. 2023. A review of the marine biogeochemical response to typhoons. Marine Pollution Bulletin, 194: 115408, doi: 10.1016/j.marpolbul.2023.115408

Chiranjeevulu G, Murty K N, Sarma N, et al. 2014. Colored dissolved organic matter signature and phytoplankton response in a coastal ecosystem during mesoscale cyclonic (cold core) eddy. Marine Environmental Research, 98: 49–59, doi: 10.1016/j.marenvres.2014.03.002

Coble P G. 1996. Characterization of marine and terrestrial DOM in seawater using excitation-emission matrix spectroscopy. Marine Chemistry, 51(4): 325–346, doi: 10.1016/0304-4203(95)00062-3

Coble P G. 2007. Marine optical biogeochemistry: the chemistry of Ocean Color. Chemical Reviews, 107(2): 402–418, doi: 10.1021/cr050350+

Conmy R N, Coble P G, Cannizzaro J P, et al. 2009. Influence of extreme storm events on West Florida shelf CDOM distributions. Journal of Geophysical Research Biogeosciences, 114(G4): G00F04, doi: 10.1029/2009JG000981

Danhiez F P, Vantrepotte V, Cauvin A, et al. 2017. Optical properties of chromophoric dissolved organic matter during a phytoplankton bloom. Implication for DOC estimates from CDOM absorption. Limnology and Oceanography, 62(4): 1409–1425, doi: 10.1002/lno.10507

Gao Lei, Gao Yongqiang, Zong Haibo, et al. 2019. Elucidating the hidden nonconservative behavior of DOM in large river-dominated estuarine and coastal environments. Journal of Geophysical Research: Oceans, 124(6): 4258–4271, doi: 10.1029/2018JC014731

Gasol J M, Vázquez-Domínguez E, Vaqué D, et al. 2009. Bacterial activity and diffusive nutrient supply in the oligotrophic central Atlantic Ocean. Aquatic Microbial Ecology, 7(1): 1–12, doi: 10.3354/ab01310

Grasshoff K, Kremling K, Ehrhardt M. 1999. Methods of Seawater Analysis. Weinheim: Wiley-VCH

Guo Weidong, Stedmon C A, Han Yuchao, et al. 2007. The conservative and non-conservative behavior of chromophoric dissolved organic matter in Chinese estuarine waters. Marine Chemistry, 107(3): 357–366, doi: 10.1016/j.marchem.2007.03.006

Guo Weidong, Yang Liyang, Hong Huasheng, et al. 2011. Assessing the dynamics of chromophoric dissolved organic matter in a subtropical estuary using parallel factor analysis. Marine Chemistry, 124(1–4): 125–133, doi: 10.1016/j.marchem.2011.01.003

Guo Weidong, Yang Liyang, Zhai Weidong, et al. 2014. Runoff-mediated seasonal oscillation in the dynamics of dissolved organic matter in different branches of a large bifurcated estuary—The Changjiang Estuary. Journal of Geophysical Research: Biogeosciences, 119(5): 776–793, doi: 10.1002/2013JG002540

Hansen A M, Kraus T E C, Pellerin B A, et al. 2016. Optical properties of dissolved organic matter (DOM): effects of biological and photolytic degradation. Limnology and Oceanography, 61(3): 1015–1032, doi: 10.1002/lno.10270

He Biyan, Dai Minhan, Zhai Weidong, et al. 2010. Distribution, degradation and dynamics of dissolved organic carbon and its major compound classes in the Pearl River Estuary, China. Marine Chemistry, 119(1–4): 52–64, doi: 10.1016/j.marchem.2009.12.006

He Guirong, Lao Qibin, Jin Guangzhe, et al. 2023. Increasing eutrophication driven by the increase of phosphate discharge in a subtropical bay in the past 30 years. Frontiers in Marine Science, 10: 1184421, doi: 10.3389/fmars.2023.1184421

He Ding, Li Penghui, He Chen, et al. 2022. Eutrophication and watershed characteristics shape changes in dissolved organic matter chemistry along two river-estuarine transects. Water Research, 214: 118196, doi: 10.1016/j.watres.2022.118196

Helms J R, Stubbins A, Ritchie J D, et al. 2008. Absorption spectral slopes and slope ratios as indicators of molecular weight, source, and photobleaching of chromophoric dissolved organic matter. Limnology and Oceanography, 53(3): 955–969, doi: 10.4319/lo.2008.53.3.0955

Hoge F E, Lyon P E. 2002. Satellite observation of chromophoric dissolved organic matter (CDOM) variability in the wake of hurricanes and typhoons. Geophysical Research Letters, 29(19): 1908, doi: 10.1029/2002GL015114

Hu Bin, Wang Peifang, Wang Chao, et al. 2022. Photogeochemistry of particulate organic matter in aquatic systems: a review. Science of the Total Environment, 806: 150467, doi: 10.1016/j.scitotenv.2021.150467

Huang Jiongqing, Zhao Huaxian, Yang Shu, et al. 2022. Mycoplanktonic community structure and their roles in monitoring environmental changes in a subtropical estuary in the Beibu Gulf. Journal of Marine Science and Engineering, 10(12): 1940, doi: 10.3390/jmse10121940

Huguet A, Vacher L, Relexans S, et al. 2009. Properties of fluorescent dissolved organic matter in the Gironde Estuary. Organic Geochemistry, 40(6): 706–719, doi: 10.1016/j.orggeochem.2009.03.002

Jiao Nianzhi, Herndl G J, Hansell D A, et al. 2010. Microbial production of recalcitrant dissolved organic matter: long-term carbon storage in the Global Ocean. Nature Reviews Microbiology, 8(8): 593–599, doi: 10.1038/nrmicro2386

Jiao Nianzhi, Tang Kai, Cai Haiyuan, et al. 2011. Increasing the microbial carbon sink in the sea by reducing chemical fertilization on the land. Nature Reviews Microbiology, 9(1): 75, doi: 10.1038/nrmicro2386-c2

Jiao Nianzhi, Wang Hong, Xu Guanhua, et al. 2018. Blue carbon on the rise: challenges and opportunities. National Science Review, 5(4): 464–468, doi: 10.1093/nsr/nwy030

Ke Sheng, Zhang Peng, Ou Shujun, et al. 2022. Spatiotemporal nutrient patterns, composition, and implications for eutrophication mitigation in the Pearl River Estuary, China. Estuarine, Coastal and Shelf Science, 266: 107749, doi: 10.1016/j.ecss.2022.107749

Lao Qibin, Chen Fajin, Jin Guangzhe, et al. 2023a. Characteristics and mechanisms of typhoon-induced decomposition of organic matter and its implication for climate change. Journal of Geophysical Research: Biogeosciences, 128(6): e2023JG007518, doi: 10.1029/2023JG007518

Lao Qibin, Liu Sihai, Ling Zheng, et al. 2023b. External dynamic mechanisms controlling the periodic offshore blooms in Beibu Gulf. Journal of Geophysical Research: Oceans, 128(6): e2023JC019689, doi: 10.1029/2023JC019689

Lao Qibin, Liu Guoqiang, Shen Youli, et al. 2021. Biogeochemical processes and eutrophication status of nutrients in the northern Beibu Gulf, South China. Journal of Earth System Science, 130(4): 199, doi: 10.1007/s12040-021-01706-y

Lao Qibin, Lu Xuan, Chen Fajin, et al. 2023c. Effects of upwelling and runoff on water mass mixing and nutrient supply induced by typhoons: insight from dual water isotopes tracing. Limnology and Oceanography, 68(1): 284–295, doi: 10.1002/lno.12266

Lao Qibin, Lu Xuan, Chen Fajin, et al. 2023d. A comparative study on source of water masses and nutrient supply in Zhanjiang Bay during the normal summer, rainstorm, and typhoon periods: insights from dual water isotopes. Science of the Total Environment, 903: 166853, doi: 10.1016/j.scitotenv.2023.166853

Lao Qibin, Wu Junhui, Chen Fajin, et al. 2022a. Increasing intrusion of high salinity water alters the mariculture activities in Zhanjiang Bay during the past two decades identified by dual water isotopes. Journal of Environmental Management, 320: 115815, doi: 10.1016/j.jenvman.2022.115815

Lao Qibin, Zhang Shuwen, Li Zhiyang, et al. 2022b. Quantification of the seasonal intrusion of water masses and their impact on nutrients in the Beibu Gulf using dual water isotopes. Journal of

Geophysical Research: Oceans, 127(7): e2021JC018065, doi: 10.1029/2021JC018065

Lawaetz A J, Stedmon C A. 2009. Fluorescence intensity calibration using the Raman scatter peak of water. Applied Spectroscopy, 63(8): 936–940, doi: 10.1366/000370209788964548

Letourneau M L, Medeiros P M. 2019. Dissolved organic matter composition in a marsh-dominated estuary: response to seasonal forcing and to the passage of a hurricane. Journal of Geophysical Research: Biogeoscience, 124(6): 1545–1559, doi: 10.1029/2018JG004982

Li Mengting, Song Guisheng, Xie Huixiang. 2022a. Bio- and photolability of dissolved organic matter in the Pearl River (Zhujiang) estuary. Marine Pollution Bulletin, 174: 113300, doi: 10.1016/j.marpolbul.2021.113300

Li Yuxuan, Yang Dezhou, Xu Lingjing, et al. 2022b. Three types of typhoon-induced upwellings enhance coastal algal blooms: a case study. Journal of Geophysical Research: Oceans, 127(5): e2022JC018448, doi: 10.1029/2022JC018448

Li Penghui, Zhao Chen, Liu Ke, et al. 2021. Anthropogenic influences on dissolved organic matter in Three Coastal Bays, North China. Frontiers in Earth Science, 9: 697758, doi: 10.3389/feart.2021.697758

Lin I I. 2012. Typhoon-induced phytoplankton blooms and primary productivity increase in the western North Pacific subtropical ocean. Journal of Geophysical Research: Oceans, 117(C3): C03039, doi: 10.1029/2011jc007626

Lin I, Liu W Timothy, Wu Chun-Chieh, 2003. New evidence for enhanced ocean primary production triggered by tropical cyclone. Geophysical Research Letters, 30(13): 1718, doi: 10.1029/2003gl017141

Liu Yuchen, Ye Quanhui, Huang Wanling, et al. 2020. Spectroscopic and molecular-level characteristics of dissolved organic matter in the Pearl River Estuary, South China. Science of the Total Environment, 710: 136307, doi: 10.1016/j.scitotenv.2019.136307

Loginova A N, Thomsen S, Engel A. 2016. Chromophoric and fluorescent dissolved organic matter in and above the oxygen minimum zone off Peru. Journal of Geophysical Research: Oceans, 121(11): 7973–7990, doi: 10.1002/2016JC011906

Lorenzen C J. 1967. Determination of chlorophyll and pheo-pigments: spectrophotometric equations. Limnology and Oceanography, 12(2): 343–346, doi: 10.4319/lo.1967.12.2.0343

Lu Xuan, Lao Qibin, Chen Fajin, et al. 2022a. Assessing the sources and dynamics of organic matter in a high human impact bay in the northern Beibu Gulf: insights from stable isotopes and optical properties. Frontiers in Marine Science, 9: 1043278, doi: 10.3389/fmars.2022.1043278

Lu Xuan, Wang Chao, Lao Qibin, et al. 2023. Interactions between particulate organic matter and dissolved organic matter in a weak dynamic bay revealed by stable isotopes and optical properties. Frontiers in Marine Science, 10: 1144818, doi: 10.3389/fmars.2023.1144818

Lu Xuan, Zhou Xin, Jin Guangzhe, et al. 2022b. Biological impact of Typhoon Wipha in the coastal area of western Guangdong: a comparative field observation perspective. Journal of Geophysical Research: Biogeosciences, 127(2): e2021JG006589, doi: 10.1029/2021JG006589

Peng Shiyun, Kong Deming, Li Liting, et al. 2020. Distribution and sources of DDT and its metabolites in porewater and sediment from a typical tropical bay in the South China Sea. Environmental Pollution, 267: 115492, doi: 10.1016/j.envpol.2020.115492

Qiu Dajun, Zhong Yu, Chen Yongqiang, et al. 2019. Short-term phytoplankton dynamics during typhoon season in and near the Pearl River Estuary, South China Sea. Journal of Geophysical Research: Biogeosciences, 124(2): 274–292, doi: 10.1029/2018JG004672

Qu Liyin, He Chen, Wu Zetao, et al. 2022. Hypolimnetic deoxygenation enhanced production and export of recalcitrant dissolved organic matter in a large stratified reservoir. Water Research, 219: 118537, doi: 10.1016/j.watres.2022.118537

Qu Liyin, Wu Yufang, Li Yan, et al. 2020. El Niño-driven dry season flushing enhances dissolved organic matter export from a subtropical watershed. Geophysical Research Letters, 47(19): e2020GL089877, doi: 10.1029/2020GL089877

Sobel A H, Camargo S J, Hall T M, et al. 2016. Human influence on tropical cyclone intensity. Science, 353(6296): 242–246, doi: 10.1126/science.aaf6574

Stedmon C A, Bro R. 2008. Characterizing dissolved organic matter fluorescence with parallel factor analysis: a tutorial. Limnology and Oceanography: Methods, 6(11): 572–579, doi: 10.4319/lom.2008.6.572

Sun Xingnian, Li Penghui, Zhou Yuping, et al. 2022. Linkages between optical and molecular signatures of dissolved organic matter along the Yangtze River Estuary-to-East China Sea continuum. Frontiers in Marine Science, 9: 933561, doi: 10.3389/fmars.2022.933561

Wang Tongyu, Chen Fajin, Zhang Shuwen, et al. 2022. Physical and biochemical responses to sequential tropical cyclones in the Arabian Sea. Remote Sensing, 14(3): 529, doi: 10.3390/rs14030529

Wang Chao, Guo Weidong, Li Yan, et al. 2017. Hydrological and biogeochemical controls on absorption and fluorescence of dissolved organic matter in the northern South China Sea. Journal of Geophysical Research: Biogeosciences, 122(12): 3405–3418, doi: 10.1002/2017JG004100

Wang Chao, Guo Weidong, Li Yan, et al. 2021a. Temperature-regulated turnover of chromophoric dissolved organic matter in global dark marginal basins. Geophysical Research Letters, 48(19): e2021GL094035, doi: 10.1029/2021GL094035

Wang Chao, Li Yizhen, Li Yan, et al. 2021b. Dissolved organic matter dynamics in the epipelagic Northwest Pacific low-latitude western boundary current system: insights from optical analyses. Journal of Geophysical Research: Oceans, 126(9): e2021JC017458, doi: 10.1029/2021JC017458

Wu Liguang, Wang Bin, Geng Shuqin. 2005. Growing typhoon influence on East Asia. Geophysical Research Letters, 32(18): L18703, doi: 10.1029/2005gl022937

Xiao Shicong, Chen Jiaxin, Shen Yuan, et al. 2023. Molecular characterization of organic matter transformation mediated by microorganisms under anoxic/hypoxic conditions. Science China: Earth Sciences, 66(4): 894–909, doi: 10.1007/s11430-022-1080-8

Yuan Xiang, Yin Kedong, Harrison P J, et al. 2010. Bacterial production and respiration in subtropical Hong Kong waters: influence of the Pearl River discharge and sewage effluent. Aquatic Microbial Ecology, 58(2): 167–179, doi: 10.3354/ame01346

Zhang Yongyu, Zhang Jihong, Liang Yantao, et al. 2017. Carbon sequestration processes and mechanisms in coastal mariculture environments in China. Science China: Earth Sciences, 60(12): 2097–2107, doi: 10.1007/S11430-017-9148-7

Zhao Hui, Shao Jinchao, Han Guoqi, et al. 2015. Influence of typhoon Matsa on phytoplankton chlorophyll-*a* off East China. PLoS One, 10(9): e0137863, doi: 10.1371/journal.pone.0137863

Zhao Hui, Tang Danling, Wang Dongxiao. 2009. Phytoplankton blooms near the Pearl River Estuary induced by Typhoon Nuri. Journal of Geophysical Research: Oceans, 114(C12): C12027, doi: 10.1029/2009JC005384

Zhao Chen, Zhou Yuping, Pang Yu, et al. 2021. The optical and molecular signatures of DOM under the eutrophication status in a shallow, semi-enclosed coastal bay in Southeast China. Science China: Earth Sciences, 64(7): 1090–1104, doi: 10.1007/s11430-020-9728-4

Zhou Xin, Jin Guangzhe, Li Jiacheng, et al. 2021. Effects of Typhoon Mujigae on the biogeochemistry and ecology of a semi-enclosed bay in the northern South China Sea. Journal of Geophysical Research: Biogeosciences, 126(7): e2020JG006031, doi: 10.1029/2020JG006031

Zsolnay A, Baigar E, Jimenez M, et al. 1999. Differentiating with fluorescence spectroscopy the sources of dissolved organic matter in soils subjected to drying. Chemosphere, 38(1): 45–50, doi: 10.1016/S0045-6535(98)00166-0

Zweifel U L, Norrman B, Hagström Å. 1993. Consumption of dissolved organic carbon by marine bacteria and demand for inorganic nutrients. Marine Ecology Progress Series, 101(1–2): 23–32, doi: 10.3354/meps101023

Supplementary information:

Fig. S1. EEM contours of fluorescent components C1–C3 identified using PARAFAC.

Fig. S2. Bottom distribution of temperature, salinity, DO, DO% and AOU in the Zhanjiang Bay during pre- and post-typhoon periods.

Fig. S3. Bottom distribution of Chl *a*, DIN ($NH_4^+ + NO_2^- + NO_3^-$), PO_4^{3-}, and SiO_3^{2-} in the Zhanjiang Bay during pre- and post-typhoon periods.

Fig. S4. Bottom distribution of a_{254}, a_{325}, and $S_{275-295}$ in the Zhanjiang Bay during pre- and post-typhoon periods.

Fig. S5. Bottom and bottom distribution of C1, C2, C3, HIX, BIX and FI in the Zhanjiang Bay during pre- and post-typhoon periods.

Fig. S6. Relationships between Chl *a* and C3 in the Zhanjiang Bay during pre- and post-typhoon. Red lines and grey shadings represent the linear fit lines and 95% confidence bands, respectively. Two data of Chl *a* were excluded from the analyses due to anomalies in their values after the typhoon.

Fig. S7. Variations of DIN (μmol/L) (a, b), PO_4^{3-} (μmol/L) (c, d), SiO_3^{2-} (μmol/L) (e, f) along with salinity in the water of Zhanjiang Bay during the pre- and post-typhoon. The red stars denote the low-salinity and high-salinity end-members used in this study.

Table S1. End-member values of salinity and DOM in low salinity end-member and high-salinity end-member during pre-typhoon

Table S2. End-member values of salinity and DOM in low salinity end-member and high-salinity end-member during post-typhoon

Table S3. Summary of the mean Chl a (μg L^{-1}), CDOM and $S_{275-295}$, FDOM and FI, HIX, and BIX values during the pre- and post-typhoon periods in Zhanjiang Bay.

Table S4. Summary of the mean temperature, salinity, dissolved oxygen, AOU, and DO saturation, nutrients values, EI during the pre- and post-typhoon periods in Zhanjiang Bay.

Table S5. The mean values of Δa_{254} (m^{-1}), Δa_{325} (m^{-1}), ΔC1 (10^{-2} RU), ΔC2 (10^{-2} RU), ΔC3 (10^{-2} RU) during the pre- and post-typhoon periods in Zhanjiang Bay.

The supplementary information is available online at https://doi.org/10.1007/s13131-023-2283-6 and http://www.aosocean.com/. The supplementary information is published as submitted, without typesetting or editing. The responsibility for scientific accuracy and content remains entirely with the authors.